UDC 621.983.1:621.979

UTJECAJ DIZAJNA ŽIGA NA PROCES OBLIKOVANJA LIMA
PUNCH DESIGN INFLUENCE ON STAMPABILITY

Ravilson Antonio CHEMIN FILHO - Paulo Victor Prestes MARCONDES

Sažetak: *Promjene su često potrebne prilikom testiranja alata za štancanje. Te promjene mogu varirati od promjena na matrici i dizajnu žiga do odabira novih materijala sa boljim karakteristikama oblikovanja. Identifikacija područja na izratku gdje istezanje, duboko vučenje i/ili ravninsko deformiranje nastaje tijekom procesa oblikovanja može dozvoliti da proces teče glatko preko optimizaciju alatne geometrije. Danas se pažnja posvećuje na ispitivanje materijala baziranog na alatnoj geometriji. U ovome radu, efekt krivulje očvršćivanja za modele žigova sa promjenjivim geometrijama su analizirane u dodatku sa tradicionalnom metodom Nakazima za ispitivanjem alata. Otkrilo se je da markirano smanjenje radijusa alata (R1 i R2 radijus) smanjuje potencijal na način da se smanjuje glavno naprezanje.*

Ključne riječi: – štancanje
– dizajn žiga
– oblikovanje metalnih ploča

Abstract: *Alterations are often necessary during the tryout of stamping tools. These changes may range from adjustments on die and punch design to the selection of a new material with better formability characteristics. The identification of regions in the workpiece where stretching, deep drawing and/or plane strain will occur during the forming process can allow the process to work smoothly through the tools' geometry optimization. Nowadays, increasing attention has focused on a material evaluation based on tool geometries. In this work, the effect on the Forming Limit Curve of four punch models with varying geometries was analyzed in addition to the traditional Nakazima test tool. It was found that a marked reduction in the tool's radiuses (R1 and R2 radii) reduces the material forming potential by decreasing the major true strain.*

Keywords: – stampability
– punch design
– sheet metal forming

1. INTRODUCTION

A perfectly compatible sheet metal formability is essential in the production of quality formed products [1, 2]. Process planners and tool designers should determine the required formability level for each piece to be stamped [3, 4]. Also the steel formability of each lot to be used in production should be evaluated.

The property of formability is difficult to determine, since there is no single parameter that will allow an overall evaluation for every stamping process [5]. Under a defined work condition, a material may be easily formable using a given tool but may tear when used in another tool with a different geometry. According to Liu *et al.* [6], the contact area between the workpiece and tools (and the tool geometry influence among them) plays an important role in deciding the forming forces and strain distribution in the formed part. These, in turn, control the incidence of failures due to cracking, wrinkling, tearing and geometric variability.

Makinouchi [7] reports that changes are often necessary in the tryout of stamping tools and they may range from the choice of a new material with improved formability to adjustments in the design of dies and punches in order to attain the level of satisfaction expected for the product. However, all these actions require time and money, creating the need for better true strain distribution knowledge during processing [8, 9].

The identification of regions of stretching, deep drawing and/or plane strain during forming can contribute to improvement in the stamping process through tool geometry optimization [10, 11]. In this context, the material's Forming Limit Curve (FLC) corresponds to the geometrical location of the maximum true strain points of a sheet subjected to stretching, deep drawing and/or plane strain condition [12]. The knowledge of the FLC is essential so that the true strain distribution produced during industrial scale does not exceed the safe deformation, thus ensuring the quality of the final product. Current research is aimed at improving Nakazima's test tools to produce more realistic results, characterizing as best as possible the phenomena acting during large plastic deformation [13, 14].

Since there rarely exists an analytical expression describing the relationships between these design parameters, dimensioning and tool manufacturing follow a series of costly trial-and-error procedures on the workshop floor [15]. Some analytical models are being developed but the construction of forming limit diagrams for particular materials is still basically experimental. Usually, sheet material formability is still evaluated through the concept of Forming Limit Curves.
In this work, the results expectation is to help the material evaluation based on the tool geometries in order to obtain an evaluation of how a differing tool design affects the material's Forming Limit Curve. As we analyzed a simple shape part, the Forming Limit Strain Diagram was chosen instead of the Forming Limit Stress Diagram, independently of the strain path [16].

2. EXPERIMENTAL PROCEDURE

The material used was a cold-rolled mild steel alloy produced by Thyssen Krupp in accordance with the DC06 specification (0.7 mm thickness). This material was selected because it has high formability properties.
For the experimental tests, four new punch models were prepared on a CNC lathe in addition to the original hemispherical punch [17]. The first punch model, cylinder-shaped, was dubbed P1 and the second model (having a shallow elliptical shape) was identified as P2. The Nakazima's [12] traditional hemispherical punch was called P3. Punch P4 showed a deep elliptical shape. The last punch model designed for these tests, dubbed P5, was shaped as an extra deep ellipse (Figure 1). The four proposed punch models were designed according to the 100 mm diameter proposed by Nakazima [12].
An important factor in the development of the geometry of each punch used in this study was the specification of the R1 and R2 radii, the former corresponding to the size of the punch head and the latter responsible for the congruence of R1 with the rectilinear portion of the tool. The congruence between these radii was the determining factor in assigning the aforementioned shapes for each punch (Figure 1).
Nakazima's test originally foresees a total of eighteen test specimens, all with a length of 200 mm and widths varying from 40 to 200 mm. This variation in the test specimens' widths is what enables the simulation of the prevailing strain modes during the test. The basic modes are: stretching, which occurs when the sample's width suffices for the full action of the drawbed around the entire contour of the stamped body and deep drawing, when the test specimen is narrower (the lateral portion of the test specimen is not held by the drawbed).
In this work, twelve test specimens were used to obtain the FLC by the traditional test method (punch P3). All the sheets were cut into 200 mm lengths and widths varying from 40, 50, 60, 70, 80, 90, 100, 110, 125, 150, 175 and 200 mm. Based on these test specimens, configurations of the sheets were prepared for two batteries of tests. The first battery of tests was aimed at defining the material FLC using the hemispherical punch (P3) and the remaining punches (P1, P2, P4 and P5), which were used in the second series of tests to evaluate the punch geometry influence.
Two kinds of test specimens (TS) were evaluated in this study, one being 200 x 200 mm (for the stretching condition) and the other 125 x 200 mm (for the deep drawing condition). Both were tested with the five punch models adopted for the tests. The tests were carried out without lubrication, a condition considered more critical in terms of friction. An average of three test specimens was evaluated for each one of the punch geometries and the results were recorded as the average of the three measurements.
It is worth mentioning that two new samples were also prepared for punch P3. The purpose of these tests was to prolong the FLC into the stretching field, using a 0.4 mm polyurethane film as a lubricant.
The reason for this was that, without lubrication, the maximum level attained for the minor true strain (ε_2) in stretching is very slight (it does not generate a complete FLC profile).
A 4.2 mm diameter grid (circles) was printed on the surface of the test specimens. This grid served to measure the true strains after stamping. The grid was printed using a new process developed during this research, which differs from the previously used processes (electrolytic, photosensitive resin or laser marking). This new marking process uses a screen (template) similar to the kind used in the silkscreen technique and a grid fixer developed for the coated metallic sheet employed. The process proved simpler, easier to apply and cheaper, since no special equipment is required for the grid imprint.
In the stamping process, the test specimens with circular grids uniformly imprinted upon them were deformed up to the point of rupture. The shape of the initial circles changed to larger circles or ellipses after forming, with greater elongation of the ellipse at the points of major true strain (Figure 2). After being deformed, the printed circles were measured with a calibrated transparent Mylar tape with diverging 'railroad tracks'. Measurements were taken of the largest axes of the circles and the largest and smallest axes of the ellipses generated according to the strain mode type.

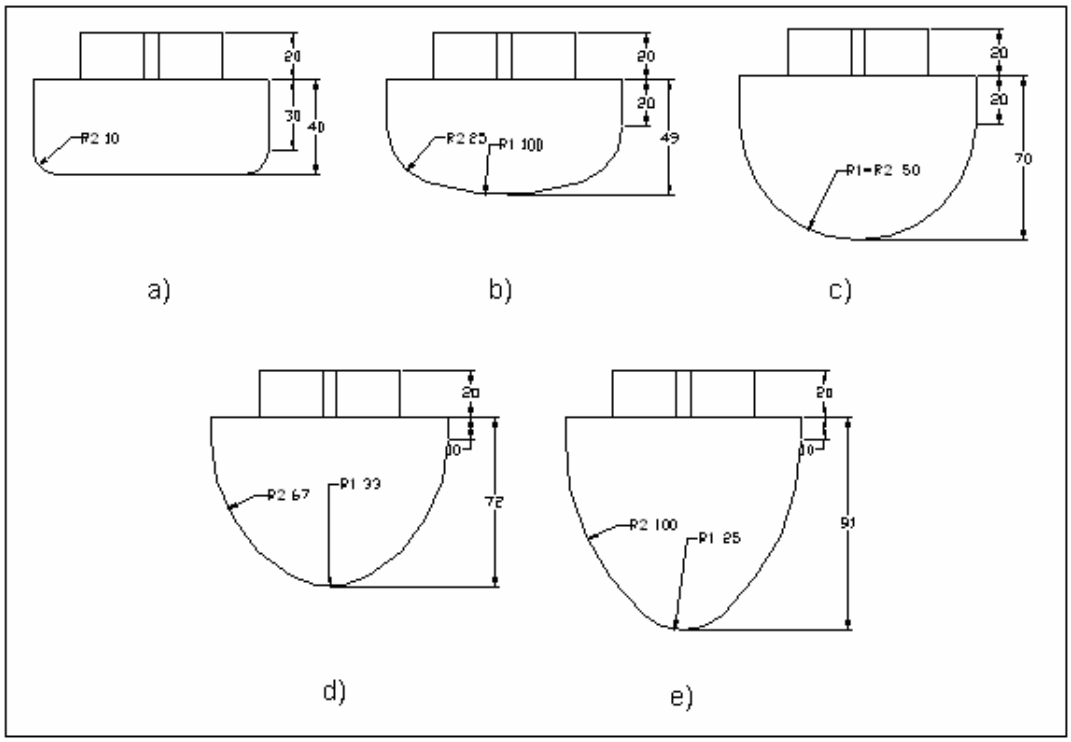

Figure 1. Punch geometry and congruence radiuses of each tool – 100 mm *diameter: a) cylindrical punch (P1), b) shallow-ellipse punch (P2), c) hemispherical punch (P3), d) deep-ellipse punch (P4) and e) extra deep-ellipse punch (P5)*

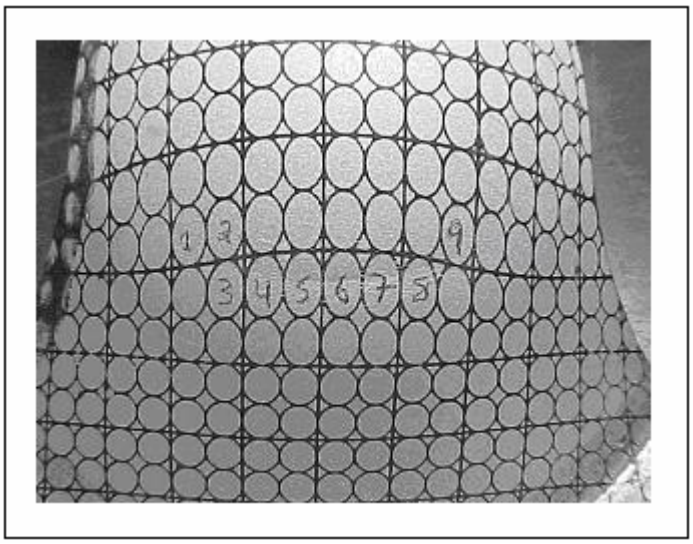

Figure 2. Test specimen showing a representative grid of circles after forming

3. RESULTS AND DISCUSSION

Figure 3a shows the FLC obtained by the traditional Nakazima testing method using the hemispherical punch (P3). The strain points measured on the specimens tested with the P1 geometry were superimposed on this curve. The results with the remaining punch geometries (P2, P4 and P5) are shown in Figures 3b to d, respectively.

As can be seen from Figure 3a, the true strain points measured on the specimens with 125 and 200 mm using

the cylindrical punch (P1) were lower than the FLC (black) measured using the hemispherical punch (P3). A maximum major true strain (ε_1) value of approximately 0.20 was reached for the cylindrical punch (P1), while the curve for the hemispherical punch (P3) reached a value of 0.32. Thus, the difference between the maximum ε_1 point and the FLC was 0.12 in the plane strain state. From the dispersion data obtained with the two different kinds of specimens (gray for the 200 x 200 mm and gray light for the 125 x 200 mm), it can be noted that the workpieces tended to present the same strain behaviour as was presented for those stamped with the hemispherical punch (P3).

The 125 mm wide workpieces exhibited a preferentially deep drawing condition, while the 200 mm wide specimens favoured the stretching behaviour. Hence, it was found that the punch geometry (P1) practically did not affect the strain mode. In other words, the 125 mm wide workpieces maintained most points in the deep drawing condition, while the 200 mm wide specimens concentrated points on the stretching condition. This finding indicates that the cylindrical punch (P1) influence is mainly in the material's stampability (which is determined by the height of the FLC) while the strain behaviour remains defined preferentially by the test specimen's geometry.

The second punch model, in the shape of a shallow ellipse (P2) corresponds to an intermediary model between the cylindrical (P1) and hemispherical (P3) shapes, Figure 3b. Geometrically, this punch model has a larger radius than the hemispherical punch, making it congruent with the radius of the punch tip. In this case, we can see a very close approximation between the major true strain points obtained with punch P2 and the FLC resulting from the tests with the hemispherical punch (P3). This similarity occurs in the plane strain state, a condition in which the minor true strain (ε_2) on the sheet is zero. Thus, the material strain occurred only in relation to the major axis (ε_1) on the sheet metal plane and is compensated by the material's thickness reduction. The point's concentration on the ε_1 axis (plane strain state) occurred with the two workpieces models studied (125 and 200 mm widths). Therefore, it can be stated that this punch model reduces the effect produced by the test specimen's geometry by distributing the points for stretching and deep drawing conditions (bringing them closer to the plane strain state).

In terms of punch geometrical variation from the cylindrical (P1) to the shallow elliptical shape (P2) and the hemispherical model (P3), there is clearly an improvement in the material's formability as a result of the contact area variation between the punch and the sheet. Thus, as the punch radius tends to increase towards the hemispherical shape (P3), the area over which the load is distributed on the material increases and becomes more uniform (which implies better stamping conditions for the sheet).

Aiming to continue analyzing the punch geometry influence, the lateral radius of the punch was even further increased, reducing the radius of the punch tip. The samples of 125 and 200 mm widths were then tested once more, using the deep elliptical (P4) and extra deep elliptical punches (P5).

The Figure 3c shows the comparison between the FLC obtained with punch P3 and the true strain points measured on the samples formed with the deep elliptical punch (P4). This new variation in the tool's geometry, i.e. a larger external radius and a smaller punch tip radius, changed the region of the test specimen where the applied loads were concentrated (with the material's fracture occurring as a direct consequence of this effect). In the case of the deep elliptical punch (P4), the major strain region (which would subsequently undergo fracture) was the portion corresponding to the punch tip rather than the area corresponding to the external punch radius (where rupture occurred with the previously tested geometries P1 and P2). The true strain points measured on the samples tested with punch P4 (Figure 3c) revealed two main characteristics. The first characteristic involved the major true strain points, which reached the same formability limit of the FLC with the hemispherical punch (black curve). The second characteristic was referred to the aspect of how the points were dispersed, i.e. they diverged completely from the plane strain state. Thus, the deep drawing and stretching forming modes were clearly defined for the both test specimens used (125 mm and 200 mm widths).

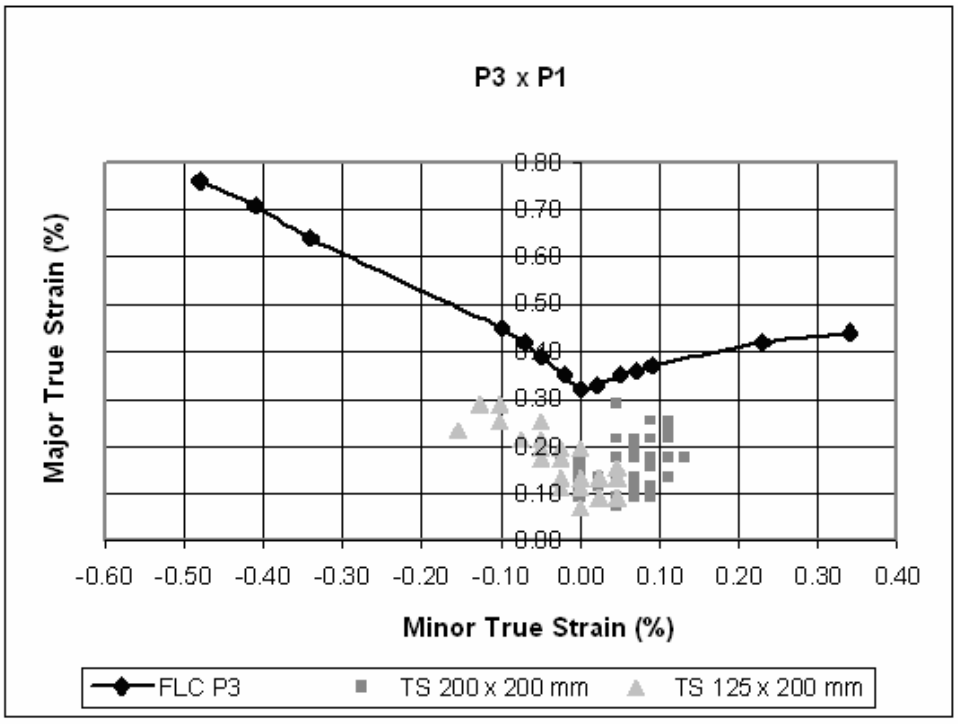
P3 x P1
Major True Strain (%)
0.80
0.70
0.60
0.50
0.40
0.30
0.20
0.10
0.00
-0.60 -0.50 -0.40 -0.30 -0.20 -0.10 0.00 0.10 0.20 0.30 0.40
Minor True Strain (%)
FLC P3
TS 200 x 200 mm
TS 125 x 200 mm

a)

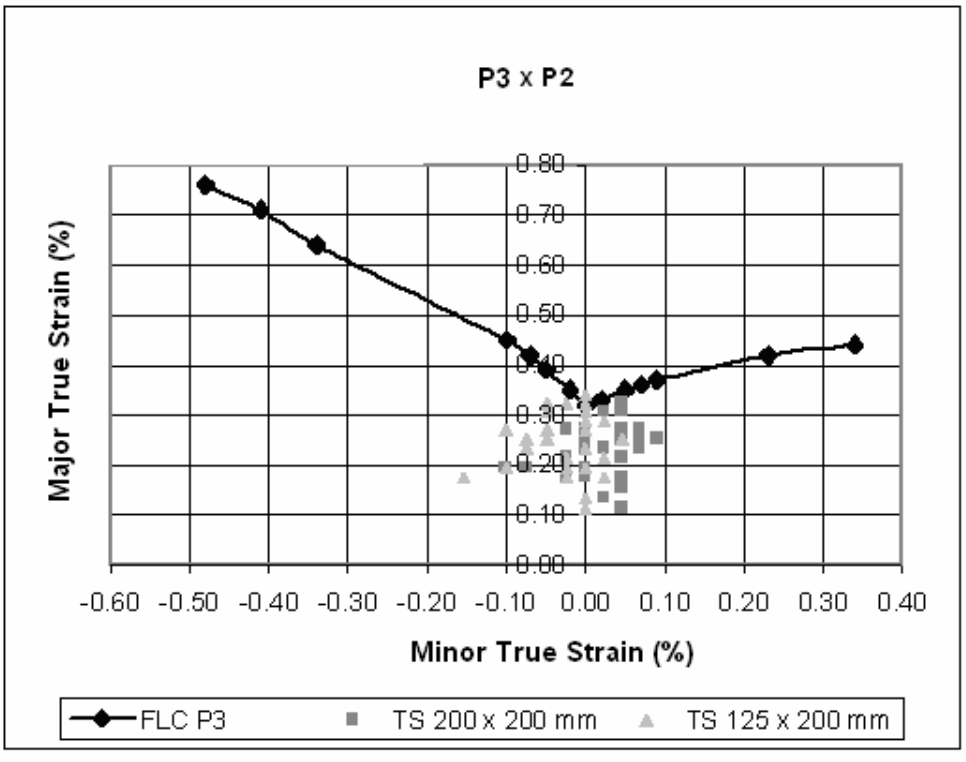
P3 x P2
Major True Strain (%)
0.80
0.70
0.60
0.50
0.40
0.30
0.20
0.10
0.00
-0.60 -0.50 -0.40 -0.30 -0.20 -0.10 0.00 0.10 0.20 0.30 0.40
Minor True Strain (%)
FLC P3
TS 200 x 200 mm
TS 125 x 200 mm

b)

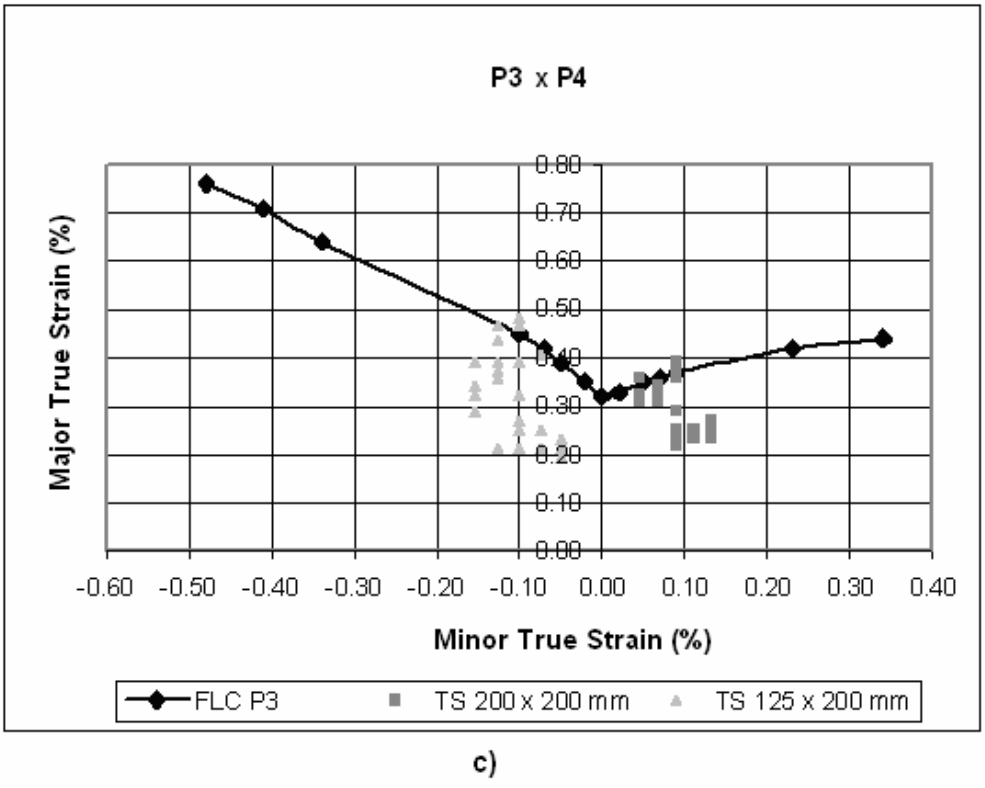

c)

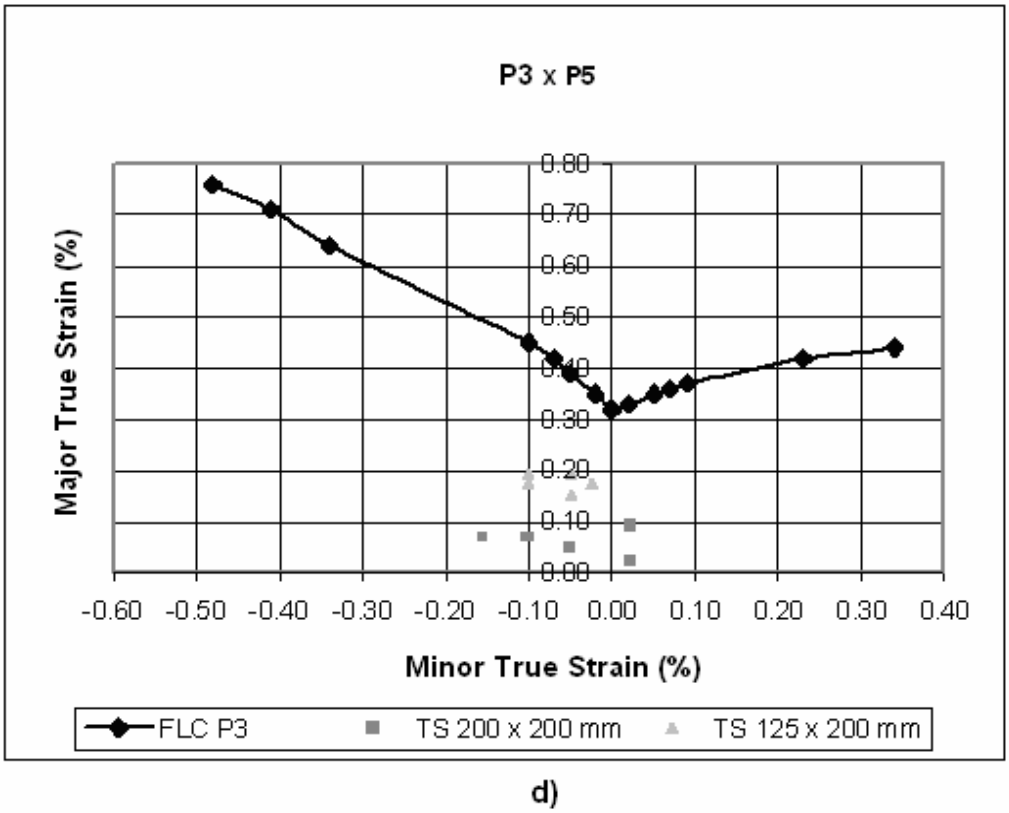

d)

Figure 3. True strain comparison (FLC) according to Nakazima and a) cylindrical punch (P1), b) shallow-ellipse punch (P2), c) deep-ellipse punch (P4) and d) extra deep-ellipse punch (P5)

The true strain effect produced by the tool geometry in the shape of an extra deep ellipse (P5) is shown in Figure 3d. This punch model was characterized principally for presenting a fairly reduced punch tip radius, thus having an increased external curved radius. The increase in the external radius was due to the need for congruence with the measure adopted for the punch tip. This tool characteristic reduced the material's formability significantly, since the points of major true strain resulting from the tests with this punch promoted true strains approximately 18 % smaller than the FLC obtained with the hemispherical punch (P3).

As in the case of the deep ellipse punch model (P4), the workpieces tested with an extra deep ellipse punch (P5) promoted strain concentrated mainly at the punch tip. Again, as in the previous case, the responsible factor for concentrating the strain at the punch tip was radius reduction in the tool region. With the punch radius even more reduced in this position, the contact area between the punch and the material was even smaller, thus increasing the stress concentration at this site. Since the punch tip radius of P5 was even smaller than that of model P4, the loads in this region were excessively concentrated. Thus, there was a drastic decrease in the values attained for the major true strain leading to lower values of stampability (compared to that reached by the material tested with the hemispherical punch). Punch P4 also promoted concentrated forces in the region of the punch tip (due to the smaller radius) but did not directly reduce the sheet metal stampability. This punch model merely promoted a better characterization of the true strain modes by deep drawing and stretching. On the other hand, punch P5 (with a smaller punch tip radius than model P4) directly affected the material's formability and an evaluation of its influence on the material's strain behaviour was precluded.

4. CONCLUSION

The results discussed herein demonstrate that the smaller the tool's radius the greater the material stress concentration, provided by the heterogeneous true strain generated, regardless of whether this radius reduction is in the outer edge or at the punch tip. It should be noted that a slight variation in the radiuses of the Nakazima's original geometry (P3) affects only the material's true strain characteristics, such as deep drawing and stretching. A marked reduction in the tool's radiuses, however, exerts an influence on the sheet formability level, i.e. it reduces the material forming potential by decreasing the major true strain.

ACKNOWLEDGMENTS

To Volkswagen do Paraná (Brazil) for supplying the samples of DC06 and to CAPES (Brazil) for a Master's grant.

REFERENCES

[1] Keeler S. P., *Understanding Sheet Metal Formability*, Machinery, 1968.

[2] Haberfield B., Boyles M. W., *Modern Concepts of Sheet Metal Formability*, Metallurgist and Materials Technologist, 1975, p. 453 - 456.

[3] Woodthorpe J. and Pearce R., *The Effect of r and n Upon the Forming Limit Diagrams of Sheet Steel*, Sheet Metal Industries, 1969, p. 1061 - 1067.

[4] Kumar D. R., *Formability analysis of extra-deep drawing steel*, Journal of Materials Processing Technology, vol. 130-131, 2002, p.31-41.

[5] Boyles M. W., Chilcott H. S., *Recent Developments in the Use of the Stretch-Draw Test*, Sheet Metal Industries. 1982, p. 149-156.

[6] Liu W. K., Hu Y-K. and Belytschko T., *ALE finite elements with hydrodynamic lubrication for metal forming*, Nuclear Engineering and Design, vol. 138, 1992, p. 1-10.

[7] Makinouchi A., *Sheet metal forming simulation in industry*, Journal of Materials Processing Technology, vol. 60, 1996, p. 19-26.

[8] Fallbohmer P., Altan T., Tonshoff H.-K. and Nakagawa T., *Survey of the die and mold manufacturing industry*, Journal of Materials Processing Technology, vol. 59, 1996, p. 158-168.

[9] Hongzhi D., Teck, C. B. Jiang, R. and Zhongqin L., *Study on geometry modeling in the dynamic stamping simulation of a die*, Journal of Materials Processing Technology, vol. 127, 2002, p. 261-265.

[10] Buchar Z., *Circle grid analysis applied to the production problems of the car body panel*, Journal of Materials Processing Technology, vol. 60, 1996, p. 205-208.

[11] Koop R., *Some current development trends in metal forming technologies*, Journal of Materials Processing Technology, vol. 60, 1996, p. 1-9.

[12] Nakazima K., Kikuma T. and Hasuka K., *Study on the Formability of Steel Sheets*, Yamata Review, 1969.

[13] Sampaio A. P., Martins C. A. and Souza P. C., *Caracterização da Conformabilidade de Aço Livre de Intersticiais – IF – Produzido via Recozimento em Caixa na Companhia Siderúrgica Nacional*, I Conferência Nacional de Conformação de Chapas, Porto Alegre, Brasil, 1998, p. 89-100 (in Portuguese).

[14] Yao H. and Cao J., *Prediction of forming limit curves using an anisotropic yield function with prestrain induced backstress*, International Journal of Plasticity, vol. 18, 2002, p. 1013-1038.
[15] Firat, M., *Computer Aided Analysis and Design of the Sheet Metal Forming Processes – Part I: The finite element modeling concepts; Part II: Deformation response modeling; Part III: Stamping die face design*, Materials & Design, 2007, p. 1298 – 1320.
[16] Gronostajski J., Matuszak A., Niechajowicz A. and Zimniak Z., *The System for Sheet Metal Forming Design of Complex Parts*, Journal of Materials Processing Technology, vol. 157-158, 2004, p. 502-507.
[17] Borsoi C. A., Hennig R. and Schaeffer L., *Novo Teste Tecnológico no LdTM para a Melhor Determinação da Conformabilidade de Chapas Metálicas*, III Conferência Nacional de Conformação de Chapas e IV Conferência Internacional de Forjamento, Porto Alegre, Brasil, 2000, p. 50-59 (in Portuguese).

Primljeno / Received: 11.3.2009.

Prihvaćeno / Accepted: 30.5.2009.

Pregledni članak

Subject review

Author's address:
Ravilson Antonio Chemin Filho
Paulo Victor Prestes Marcondes
Universidade Federal do Paraná
DEMEC
Av. Cel. Francisco H. dos Santos, 210
CEP 81531-990
Curitiba - Paraná
Brazil
ravilson@pop.com.br
marcondes@ufpr.br